Chinese Journal of
POLYMER SCIENCE

RESEARCH ARTICLE

https://doi.org/10.1007/s10118-023-2991-6
Chinese J. Polym. Sci. **2023**, *41*, 1543–1554

Synthesis of Helical Poly(phenylacetylene)s Carrying Dendritic Pendants with Varied Branching Densities Through Polymerization in Different Solvents

Zhen-Zhen Sun†, Yan-Ning Zhang†, Hao-Yu Qiu, Xue-Ting Lu, Liang-Xuan Ren, Le-Fei Shen, Wen Li*, and Afang Zhang*

International Joint Laboratory of Biomimetic and Smart Polymers, School of Materials Science and Engineering, Shanghai University, Shanghai 200444, China

Electronic Supplementary Information

Abstract Helical poly(phenylacetylene)s (PPAs) have received extensive attention because of their features in dynamic chirality and promising applications. Therefore, understanding relationship among the polymer molecular structures, polymerization conditions and tunability of their chirality is of key scientific value. Recently, we developed a novel class of dendronized PPAs carrying 3-fold dendritic oligo(ethylene glycols) (OEGs) *via* alanine linkage, and found that these bulky polymers exhibited tunable helical conformations through thermally-mediated dehydration and aggregation. Herein, we report on synthesis of a homologous series of dendronized PPAs that carry 2-fold, 3-fold or 6-fold dendritic OEG pendants, and focus on effects of molecular topological structures, peripheral units and polymerization solvents on the thermoresponsiveness and their conformation switching behaviors. Effects of branching density and peripheral units (ethoxyl or methoxyl) of the dendritic OEG pendants were examined, and found to play a decisive role on the helical conformation and thermoresponsiveness of these dendronized PPAs due to their different bulkiness and overall hydrophilicity. In addition, different polymerization solvents were checked for their possible influence on the polymerization, thermoresponsive behavior and the chirality of the resulting polymers. For polymerization in selective solvents like water or methanol, the obtained dendronized PPAs exhibited weak thermal transitions, while polymerization in non-selective solvent like THF furnished PPAs with characteristic thermoresponsive behavior, indicating that solvents were involved in the process of polymerization of the dendronized macromonomers. More interestingly, different chiralities of the PPAs through polymerization in various solvents were retained, irrelevant to the purification process and solvents treatments. This work suggests that the topological structures together with polymerization solvents can modulate the thermoresponsive behavior and helical conformation of the dendronized PPAs.

Keywords Helical polymer; Dendronized polymer; Thermoresponsive polymer; Solvation; Dendritic oligoethylene glycol

Citation: Sun, Z. Z.; Zhang, Y. N.; Qiu, H. Y.; Lu, X. T.; Ren, L. X.; Shen, L. F.; Li, W.; Zhang, A. Synthesis of helical poly(phenylacetylene)s carrying dendritic pendants with varied branching densities through polymerization in different solvents. *Chinese J. Polym. Sci.* **2023**, *41*, 1543–1554.

INTRODUCTION

Helical polymers have formed a class of intriguing polymer materials for applications ranging from chiral recognitions and chiral separations to chiro optics.[1–5] Various helical polymers have been reported, and different ways to effectively enhance or switch their helical conformation were investigated.[6–12] Through introducing amino acid units into side groups, polymers such as poly(phenylacetylene)s (PPAs) and polyisocyanides have been afforded successfully helical conformations. Chiralities of the helical polymers have been found to be dependent on molecular structures, topological structures, polymerization conditions, as well as external stimuli.[13–15] Pioneering work has revealed that stability of helical conformation for a polymer is dominated by its structural inversion barrier, therefore, helical polymers are usually divided into static helical polymers with high barriers and dynamic helical polymers with low barriers.[16] The typical static helical polymers are polyisocyanides, polytriphenyl methacrylates and polychloral derivatives. These polymers exhibit high stable helical conformations in different external conditions, such as solvents, temperature and pH, mainly because of strong steric hindrance from their large volume side groups. Even when external conditions changed, their secondary structures can still be relatively stable, although sometimes its pitch may have a little change.[17–20] For dynamic helical polymers, their main chain helicities were induced by chiral pendants through either covalent or non-covalent linkages, whose chiralities are

* Corresponding authors, E-mail: wli@shu.edu.cn (W.L.)
E-mail: azhang@shu.edu.cn (A.Z.)
† These authors contributed equally to this work.
Special Issue: Celebrating the 70th Anniversary of the Establishment of Polymer Program at Peking University
Received April 1, 2023; Accepted April 17, 2023; Published online June 12, 2023

switchable according to external stimuli.[21–24] PPAs are a typical class of dynamic helical polymers, which have excellent properties and broad application prospects in photoelectronic devices, sensors and molecular devices.[25] The small barriers for PPA chains to invert their conformations have made these polymers promising as smart chiral materials. Therefore, diversified conformation switching strategies have been applied to modulate helical conformation of PPAs, including molecular structure design and polymerization process controlling,[26–28] as well as external stimuli such as temperature,[29–31] pH,[32,33] solvents,[34–36] anions,[37–39] and mechanical force.[40–42] Even polymerization solvents were found to play an important role in mediating chiralities of the resulting PPAs.[43]

Conventional helical polymers are too hydrophobic and thus not water-soluble, which render them difficulties in applications as biomaterials in water.[13,17,32] Therefore, water-soluble or even stimuli-responsive helical polymers have received attention.[25,31,39,44] Among all stimuli-responsive helical polymers, thermoresponsive helical polymers are attractive due to their thermally switchable water-solubilities and promising applications as chiral separation and bio-functional materials.[45–47] Temperature as a stimulus is clean and can be easily controlled. By using the temperature as a tool, helicities of the polymers can be manipulated, which leads to form a novel class smart helical polymers with tunable chiralities according to thermal dehydration and rehydration.

Recently, we initiated to develop a series of dendronized PPAs carrying 3-fold dendritic oligo(ethylene glycols) (OEGs) through alanine linkage.[31] These dendronized PPAs showed characteristic thermoresponsive behavior with fast and sharp phase transitions without obvious hysteresis. Helical conformation of these PPAs can be effectively switched not only by changing solution temperatures below or above their cloud point temperatures (T_{cp}s), but also through presence of different anions.[39] Interestingly, terminal units in the peripheries of dendritic OEGs, which are far away from the polymer backbones, even exhibited significant influence on the chirality inductions during the thermally-induced phase transitions.[44] To understand the dendritic topological effects on the chirality of the dendronized PPAs and their chirality transitions during the thermal aggregation process, we here report on synthesis of a homologous series of dendronized PPAs which carry 2-fold, 3-fold and 6-fold dendritic OEG pendants with ethoxyl or methoxyl terminals (Fig. 1), aiming at exploring the dendritic topological effects. These dendronized PPAs were obtained through polymerization in different solvents, to examine possible effects of polymerization solvents on chiralities of the resulting PPAs. Their thermoresponsiveness was investigated with turbidity measurements with UV-Vis spectroscopy, chirality transformation was followed with circular dichroism (CD) measurements.

EXPERIMENTAL

General Consideration

Compounds **2a**,[48] **2b**,[48] **6**[48] and perfluorophenyl 4-ethynylbenzoate,[44] as well as monomers **Me-PA$_3$**[44] and **Et-PA$_3$**[44] and polymers **Me-PPA$_{3T}$**[44] and **Et-PPA$_{3T}$**[44] were synthesized according to our previous reports. Dichloromethane (DCM) was distilled from CaH_2. Tetrahydrofuran (THF) was distilled from $LiAlH_4$ and Na. All reactions were run under a nitrogen atmosphere. Other reagents and solvents were of reagent grade and used without further purification. Macherey-Nagel precoated TLC plates (silica gel 60 G/UV254, 0.25 mm) were used for thin-layer chromatography (TLC) analysis. Silica gel 60 M (Macherey-Nagel, 0.040–0.063 mm, 200–300 mesh) was used as the stationary phase for column chromatography.

Instruments and Measurements

^{1}H-NMR spectra were recorded on a Bruker AV 500 (^{1}H: 500 MHz) spectrometer. Gel permeation chromatography (GPC) measurements were performed on a Waters GPC e2695 instrument with a three-column set (Styragel HR3 + HR4 + HR5) equipped with a refractive index detector (Waters 2414). The calibration was performed with poly(methyl methacrylate) standards of molar masses in the range of M_p = 2540–936000 (Polymer Standards Service-USA, Inc.). DMF (containing LiBr of 1 g·L^{-1}) was used as eluent at 45 °C. CD measurements were

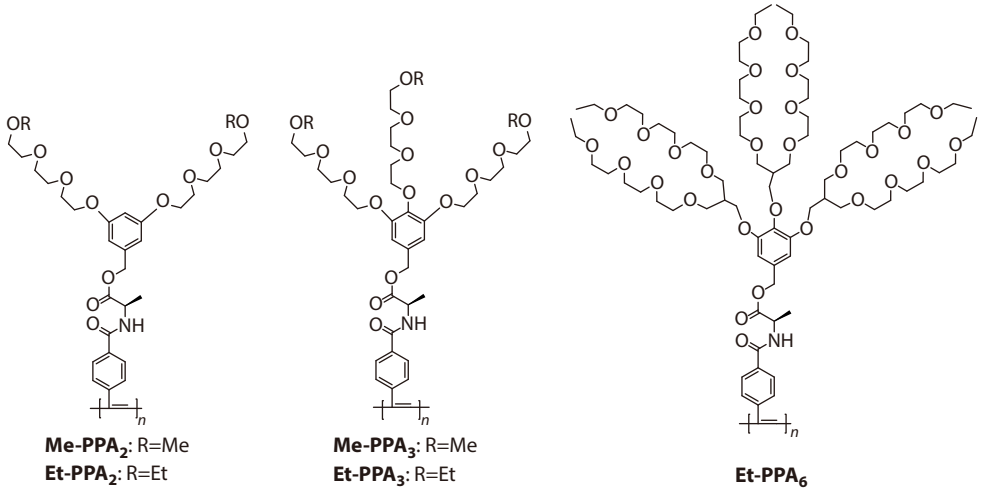

Fig. 1 Molecular structures of dendronized PPAs carrying 2-fold (**Me-PPA$_2$** and **Et-PPA$_2$**), 3-fold (**Me-PPA$_3$** and **Et-PPA$_3$**) and 6-fold (**Et-PPA$_6$**) dendritic OEGs, respectively.

https://doi.org/10.1007/s10118-023-2991-6

performed on a JASCO J-815 spectropolarimeter with a thermo-controlled 1 mm quartz cell (three accumulations, "continue scanning" mode, scanning speed: 200 nm·min^{-1}; data pitch: 0.2 nm; response: 1 s; bandwidth: 2.0 nm). UV-Vis spectroscopy and turbidity measurements were performed on a JASCO UV/Vis spectrophotometer (V-750). Aqueous polymer solutions were placed in the spectrophotometer (path length 1 cm) and heated or cooled at a rate of 0.2 °C·min^{-1}. Absorptions of the solutions at λ=700 nm were recorded per 5 s. The cloud point temperature (T_{cp}) was determined to be the one at which transmittance at λ=700 nm reached 50% of its initial value. Dynamic light scattering (DLS) experiments were performed on Wyatt Nanostarinstrument (scattering angle, 90°). The dust-free solutions of polymers were prepared by filtering through 0.45 μm Nylon filters.

*Compound **3a***

Compound **2a** (18.3 g, 57.5 mmol), 3,5-dihydroxybenzoic acid (4.2 g, 24.9 mmol) and K_2CO_3 (34.5 g, 249.6 mmol) were dissolved in dry DMF (50 mL) at 80 °C under N_2 atmosphere. The reaction mixture was stirred for 24 h. TLC was used to follow the reaction completion. Then solvent DMF was removed by rotating evaporation. The residue was dissolved in DCM and washed successively with saturated sodium chloride and deionized water. After drying over anhydrous sodium sulfate, the organic phase was filtrated and the solvent was removed by evaporation. After purification by column chromatography with DCM/MeOH (DCM/MeOH, 100/1) as the eluent, compound **3a** was obtained as colorless oil (10.4 g, 90%). ^{1}H-NMR ($CDCl_3$, δ, ppm): 3.37 (s, 6H, CH_3), 3.52–3.87 (m, 20H, CH_2), 3.89 (s, 3H, CH_3), 4.11–4.16 (m, 4H, CH_2), 6.69 (t, 1H, Ar-H), 7.18 (d, 2H, Ar-H).

*Compound **3b***

Similar as **3a** from **2b** (30 g, 90.25 mmol), 3,5-dihydroxybenzoic acid (6.6 g, 39.3 mmol) and K_2CO_3 (54.2 g, 392.2 mmol), compound **3b** was afforded as colorless oil (16.3 g, 85%). ^{1}H-NMR ($CDCl_3$, δ, ppm): 1.2 (t, 6H, CH_3), 3.48–3.87 (m, 24H, CH_2), 3.89 (s, 3H, CH_3), 4.11–4.16 (m, 4H, CH_2), 6.69 (t, 1H, Ar-H), 7.18 (d, 2H, Ar-H).

*Compound **4a***

Compound **3a** (10.4 g, 22.5 mmol), $LiAlH_4$ (1.19 g, 31.4 mmol) were dispersed in dry THF (30 mL) at 0 °C under N_2 atmosphere. The reaction mixture was stirred for 24 h. TLC was used to follow the reaction. The reaction was terminated by dropping slowly water and 10% NaOH aqueous solutions under the ice bath until clear liquid appeared in the upper layer and precipitation appeared in the lower layer. Then, the precipitation was filtered out and the THF was removed by evaporation. The residual was dissolved in DCM and washed with brine. After the organic phase was dried over $MgSO_4$, purification by column chromatography with DCM/MeOH (DCM/MeOH, 60/1) as eluent, compound **4a** was obtained as colorless oil (8.4 g, 86%). ^{1}H-NMR ($CDCl_3$, δ, ppm): 3.37 (s, 6H, CH_3), 3.51–4.13 (m, 24H, CH_2), 4.60 (s, 2H, CH_2), 6.41 (t, 1H, Ar-H), 6.53 (d, 2H, Ar-H).

*Compound **4b***

Similar as **4a** from **3b** (16.3 g, 33.4 mmol) and $LiAlH_4$ (1.8 g, 47.4 mmol), compound **4b** was afforded as colorless oily substance (13.6 g, 88%). ^{1}H-NMR ($CDCl_3$, δ, ppm): 1.2 (t, 6H, CH_3), 3.43–4.17 (m, 28H, CH_2), 4.60 (s, 2H, CH_2), 6.41 (t, 1H, Ar-H), 6.53 (d, 2H, Ar-H).

*Compound **5a***

Compound **4a** (8.4 g, 19.4 mmol), L-Boc-Ala-OH (4.8 g, 25.3 mmol) and DMAP (0.7 g, 5.7 mmol) were dissolved in DCM (50 mL) at 0 °C and N_2 atmosphere. EDC·HCl (9.3 g, 48.5 mmol) was slowly added to the solution through a constant pressure funnel. The reaction mixture was stirred for another 12 h at room temperature. After washed with saturated sodium chloride solution and deionized water, the organic phase was dried over anhydrous sodium sulfate. After filtration, the solvent was removed by evaporation. Column chromatography with DCM/MeOH (DCM/MeOH, 90/1) as eluent afforded the intermediate as colorless oil (9.2 g, 79%). Then the colorless oil was dissolved in dry DCM, and TFA (16.7 mL, 225.4 mmol) was slowly added. The mixture was stirred for another 12 h. TLC was used to follow the reaction. After quenching the reaction with slowly addition of methanol at 0 °C, evaporation of solvents yielded compound **5a** as colorless oil (5.7 g, 74%). ^{1}H-NMR (DMSO-d_6) of the intermediate with Boc: δ=1.21–1.31 (m, 3H, CH_3), 1.37 (s, 9H, CH_3), 3.23 (s, 6H, CH_3), 3.37–3.78 (m, 20H, CH_2), 4.00–4.12 (m, 4H, CH_2), 5.03 (s, 2H, CH_2), 6.46 (t, 1H, Ar-H), 6.51 (d, 2H, Ar-H), 7.36 (d, 1H, NH).

*Compound **5b***

Similar as for **5a** from compound **4b** (13.6 g, 29.5 mmol), L-Boc-Ala-OH (6.7 g, 35.4 mmol), DMAP (1.1 g, 9.0 mmol), and TFA (35.0 mL, 471.2 mmol), compound **5b** was afforded as colorless oil (10.3 g, 82%). ^{1}H-NMR ($CDCl_3$) of the intermediate with Boc: δ = 1.20 (t, 6H, CH_3), 1.39 (d, 3H, CH_3), 1.43 (s, 9H, CH_3), 3.47–4.13 (m, 28H, CH_2), 4.31–4.40 (m, 1H, CH), 5.06 (t, 2H, CH_2), 6.44 (t, 1H, Ar-H), 6.49 (d, 2H, Ar-H).

*Monomer **Me-PA$_2$***

Compound **5a** (5.7 g, 11.3 mmol) and DIEA were dissolved in dry DCM (20 mL) at 0 °C under N_2 atmosphere, and perfluorophenyl 4-ethynylbenzoate (4.6 g, 14.7 mmol) was slowly added. The mixture was stirred for another 12 h, and TLC was used to follow the reaction. After evaporation of the solvents, the residue was dissolved in DCM and washed with brine. The organic phase was dried over $MgSO_4$. Purification by chromatography using DCM as eluent afforded monomer **Me-PA$_2$** as white solid (5.8 g, 82%). ^{1}H-NMR (DMSO-d_6, δ, ppm): 1.44 (d, 3H, CH_3), 3.23 (s, 6H, CH_3), 3.39–4.06 (m, 24H, CH_2), 4.38 (s, 1H, CH), 4.53 (p, 1H, CH), 5.06 (s, 2H, CH_2), 6.44 (t, 1H, Ar-H), 6.49 (d, 2H, Ar-H), 7.54–7.63 (m, 2H, Ar-H), 7.83–7.95 (m, 2H, Ar-H), 8.95 (d, 1H, NH).

*Monomer **Et-PA$_2$***

Compound **5b** (10.3 g, 19.4 mmol) and DIEA were dissolved in dried DCM (20 mL) at 0 °C under N_2 atmosphere, and perfluorophenyl 4-ethynylbenzoate (6.7 g, 21.5 mmol) was slowly added. The reaction mixture was stirred for another 12 h and TLC was used to follow the reaction. After evaporation of the solvents, the residue was dissolved in DCM and washed with brine. The organic phase was dried over $MgSO_4$. Purification by column chromatography using DCM as eluent afforded the monomer **Et-PA$_2$** as white solid (7.9 g, 51%). ^{1}H-NMR (DMSO-d_6, δ, ppm): 1.08 (t, 6H, CH_3), 1.44 (d, 3H, CH_3), 3.37–4.07 (m, 28H, CH_2), 4.38 (s, 1H, CH), 4.54 (p, 1H, CH), 5.06 (s, 2H, CH_2), 6.44 (t, 1H, Ar-H)，6.49 (d, 2H, Ar-H), 7.55–7.62 (m, 2H, Ar-H), 7.87–7.92 (m, 2H, Ar-H), 8.95 (d, 1H, NH).

*Compound **7***

Compound **6** (4.0 g, 2.9 mmol), L-Boc-Ala-OH (0.8 g, 4.3 mmol) and DMAP (0.2 g, 1.5 mmol) were dissolved in DCM (50 mL) at

https://doi.org/10.1007/s10118-023-2991-6

0 °C under N_2 atmosphere, and EDC·HCl (1.4 g, 7.2 mmol) was slowly added through a constant pressure funnel. The mixture was stirred for another 12 h at room temperature (rt). After washed with saturated sodium chloride solution and deionized water, the organic phase was dried over anhydrous sodium sulfate. After filtration, the solvent was removed by evaporation. Column chromatography with DCM/MeOH (DCM/MeOH, 80/1) as eluent afforded the intermediate colorless oil (4.1 g, 91%). Then colorless oil was dissolved in dry DCM, and TFA (7.9 mL, 106.4 mmol) was slowly added. The mixture was stirred for another 12 h. TLC was used to follow the reaction. After quenching the reaction with slowly addition of methanol at 0 °C, the solvents were evaporated. The residue was dissolved in DCM and washed with brine. The organic phase was dried over $MgSO_4$, evaporation of solvents afforded compound **7** as colorless oil (3.4 g, 90%). ^{1}H-NMR ($CDCl_3$) of the intermediate with Boc: δ = 1.17–1.22 (m, 18H, CH_3), 1.35–1.40 (br, 3H, CH_3), 2.25–2.44 (br, 3H, CH), 3.47–3.68 (m, 96H, CH_2), 3.93–4.03 (br, 6H, CH_2), 4.76–4.83 (br, 1H, CH), 5.04–5.13 (br, 2H, CH_2), 6.54 (s, 2H, Ar-H), 6.95–6.97 (d, 1H, NH), 7.53–7.56 (br, 2H, Ar-H), 7.77–7.80 (br, 2H, Ar-H).

Monomer ***Et-PA$_6$***

Compound **7** (3.4 g, 2.3 mmol) and DIEA were dissolved in dried DCM (20 mL) at 0 °C under N_2 atmosphere, and perfluorophenyl 4-ethynylbenzoate (0.8 g, 2.6 mmol) was slowly added. The reaction mixture was stirred for another 12 h, and TLC board was used to follow the reaction. After evaporation of the solvents, the residue was dissolved in DCM and washed with brine. The organic phase was dried over $MgSO_4$. Purification by column chromatography using DCM as eluent afforded the monomer **Et-PA$_6$** as yellow oil (3.1 g, 83%). ^{1}H-NMR ($CDCl_3$, δ, ppm): 1.17–1.22 (m, 18H, CH_3), 1.51–1.54 (br, 3H, CH_3), 2.28–2.44 (br, 3H, CH), 3.21 (s, 1H, CH), 3.48–3.68 (m, 96H, CH_2), 3.92–4.03 (br, 6H, CH_2), 4.21–4.35 (br, 1H, CH), 4.95–5.10 (br, 2H, CH_2), 6.52 (s, 2H, Ar-H).

Polymer ***Me-PPA$_{2T}$***

The polymerization was performed in THF (0.4 mL) from **Me-PA$_2$** (100 mg, 0.158 mmol), $[Rh(nbd)Cl]_2$ (0.22 mg, 0.0005 mmol) and triethylamine (TEA, 0.08 mL), and the polymer was yielded as yellow solid (72 mg, 72%). ^{1}H-NMR (DMSO-d_6, 80 °C, δ, ppm) 1.35 (m, 3H, CH_3), 3.19 (s, 6H, CH_3), 3.30–3.75 (m, 20H, CH_2), 4.00 (t, 4H, CH_2), 4.51 (br, 1H, CH), 4.98 (br, 1H, CH), 5.74 (br, 2H, CH_2), 6.41 (s, 1H, Ar-H), 6.44 (d, 2H, Ar-H), 6.73 (br, 2H, Ar-H), 7.52 (br, 2H, Ar-H), 8.11 (br, 1H, NH).

Polymer ***Et-PPA$_{2T}$***

The polymerization was performed in THF (0.4 mL) from **Me-PA$_2$** (100 mg, 0.152 mmol), $[Rh(nbd)Cl]_2$ (0.23 mg, 0.0005 mmol) and TEA (0.06 mL), and the polymer was yielded as yellow solid (62 mg, 60%). ^{1}H-NMR (DMSO-d_6, 80 °C, δ, ppm): 1.04 (t, 6H, CH_3), 1.30–1.41 (m, 3H, CH_3), 3.27–3.74 (m, 24H, CH_2), 3.88–4.12 (m, 4H, CH_2), 4.51 (br, 1H, CH), 4.97 (br, 1H, CH), 5.74 (br, 2H, CH_2), 6.41 (s, 1H, Ar-H), 6.44 (s, 2H, Ar-H), 6.73 (br, 2H, Ar-H), 7.52 (br, 2H, Ar-H), 8.12 (br, 1H, NH).

Polymer ***Me-PPA$_{3W}$***

The polymerization was performed in water (0.4 mL) from **Me-PA$_3$** (200 mg, 0.252 mmol), $[Rh(nbd)Cl]_2$ (0.387 mg, 0.0008 mmol) and TEA (0.1 mL), and the polymer was yielded as yellow solid (170 mg, 85%). ^{1}H-NMR (DMSO-d_6, 80 °C, δ, ppm): 1.35 (m, 3H, CH_3), 3.20 (d, 9H, CH_3), 3.33–4.07 (m, 36H, CH_2), 4.49 (br, 1H, CH), 4.96 (br, 2H, CH_2), 5.72 (br, 1H, CH), 6.58 (s, 2H, Ar-H), 6.74 (br, 2H, Ar-H), 7.53 (br, 2H, Ar-H), 8.11 (br, 1H, NH).

Polymer ***Me-PPA$_{3M}$***

The polymerization was performed in MeOH (0.4 mL) from **Me-PA$_3$** (200 mg, 0.252 mmol), $[Rh(nbd)Cl]_2$ (0.387 mg, 0.0008 mmol) and TEA (0.1 mL), and the polymer was yielded as yellow solid (142 mg, 71%). ^{1}H-NMR (DMSO-d_6, 80 °C, δ, ppm): 1.35 (m, 3H, CH_3), 3.20 (d, 9H, CH_3), 3.29–4.14 (m, 36H, CH_2), 4.49 (br, 1H, CH), 4.96 (br, 2H, CH_2), 5.72 (br, 1H, CH), 6.58 (s, 2H, Ar-H), 6.74 (br, 2H, Ar-H), 7.53 (br, 2H, Ar-H), 8.11 (br, 1H, NH).

Polymer ***Et-PPA$_{3W}$***

Similar as that for **Et-PPA$_{3T}$**, the polymerization was performed in water (1 mL) from **Et-PA$_3$** (500 mg, 0.6 mmol), $[Rh(nbd)Cl]_2$ (0.7 mg, 0.002 mmol) and TEA (0.25 mL), and the polymer was yielded as yellow solid (471 mg, 94%). ^{1}H-NMR (Gd_6-DMSO, 80 °C, δ, ppm): 1.0–1.13 (m, 9H, CH_3), 1.25–1.30 (br, 3H, CH_3), 3.35–3.79 (m, 38H, CH_2), 3.97–4.12 (br, 6H, CH_2), 4.42 (br, 1H, CH), 4.85–5.07 (br, 2H, CH_2), 5.75 (br, 1H, CH), 6.56–6.65 (s, 2H, Ar-H), 6.90 (br, 2H, Ar-H), 7.54 (br, 2H, Ar-H), 8.14 (br, 1H, NH).

Polymer ***Et-PPA$_{3M}$***

Similar as that for **Et-PPA$_{3T}$**, the polymerization was performed in MeOH (1 mL) from **Et-PA$_3$** (500 mg, 0.6 mmol), $[Rh(nbd)Cl]_2$ (0.7 mg, 0.002 mmol) and TEA (0.25 mL), and the polymer was yielded as yellow solid (445 mg, 89%). ^{1}H-NMR (DMSO-d_6, 80 °C, δ, ppm): 0.99–1.10 (m, 9H, CH_3), 1.30–1.40 (br, 3H, CH_3), 3.33–3.75 (m, 38H, CH_2), 3.96–4.08 (br, 6H, CH_2), 4.49 (br, 1H, CH), 4.87–5.05 (br, 2H, CH_2), 5.73 (br, 1H, CH), 6.58 (s, 2H, Ar-H), 6.74 (br, 2H, Ar-H), 7.53 (br, 2H, Ar-H), 8.13 (br, 1H, NH).

Polymer ***Et-PPA$_{6T}$***

Similar as that for **Et-PPA$_{3T}$**, the polymerization was performed in THF (0.4 mL) from **Et-PA$_6$** (80 mg, 0.05 mmol), $[Rh(nbd)Cl]_2$ (0.07 mg, 0.0002 mmol) and TEA (0.02 mL), and the polymer was yielded as orange-red solid (70 mg, 87%). ^{1}H-NMR (DMSO-d_6, 80 °C, δ, ppm): 1.0–1.13 (m, 18H, CH_3), 1.34–1.42 (br, 3H, CH_3), 1.99–2.30 (br, 3H, CH), 3.32–3.63 (m, 96H, CH_2), 3.84–4.04 (br, 6H, CH_2), 4.55 (br, 1H, CH), 4.85–5.16 (br, 2H, CH_2), 5.35 (br, 1H, CH), 6.52–6.68 (s, 2H, Ar-H), 7.14–7.25 (br, 2H, Ar-H), 7.37–7.47 (br, 2H, Ar-H).

Polymer ***Et-PPA$_{6W}$***

Similar as that for **Et-PPA$_{3W}$**, the polymerization was performed in water (0.4 mL) from **Et-PA$_6$** (80 mg, 0.05 mmol), $[Rh(nbd)Cl]_2$ (0.07 mg, 0.0002 mmol) and TEA (0.02 mL), and the polymer was yielded as orange-red solid (73 mg, 91%). ^{1}H-NMR (DMSO-d_6, 80 °C, δ, ppm): 0.99–1.13 (m, 18H, CH_3), 1.35–1.45 (br, 3H, CH_3), 1.99–2.32 (br, 3H, CH), 3.29–3.69 (m, 96H, CH_2), 3.82–4.09 (br, 6H, CH_2), 4.51 (br, 1H, CH), 4.82–5.17 (br, 2H, CH_2), 5.70 (br, 1H, CH), 6.53–6.84 (s, 2H, Ar-H), 7.14–7.25 (br, 2H, Ar-H), 7.36–7.63 (br, 2H, Ar-H), 8.08 (br, 1H, NH).

Polymer ***Et-PPA$_{6M}$***

Similar as that for **Et-PPA$_{3M}$**, the polymerization was performed in MeOH (0.4 mL) from **Et-PA$_6$** (80 mg, 0.05 mmol), $[Rh(nbd)Cl]_2$ (0.07 mg, 0.0002 mmol) and TEA (0.02 mL), and the polymer was yielded as orange-red solid (71 mg, 89%). ^{1}H-NMR (DMSO-d_6, 80 °C, δ, ppm): 0.98–1.13 (m, 18H, CH_3), 1.33–1.44 (br, 3H, CH_3), 1.90–2.31 (br, 3H, CH), 3.34–3.72 (m, 96H, CH_2), 3.86–4.07 (br, 6H, CH_2), 4.50 (br, 1H, CH), 4.81–5.08 (br, 2H, CH_2), 5.71 (br, 1H, CH), 6.39–6.55 (s, 2H, Ar-H), 6.79–6.98 (br, 2H, Ar-H), 7.42–7.62 (br, 2H, Ar-H), 8.56 (br, 1H, NH).

https://doi.org/10.1007/s10118-023-2991-6

RESULTS AND DISCUSSION

Synthesis and Characterization of the Dendronized Macromonomers

A homologous series of dendronized PAs were designed and synthesized as outlined in Scheme 1. These macromonomers all carried the first generation of dendritic OEGs, which are different in their terminals (either ethoxyl or methoxyl) and branching densities (either 2-fold, 3-fold or 6-fold). For clarity, the branching density was marked as a footnote in naming the corresponding polymers. These structure variations were designed to afford the corresponding polymers with different overall hydrophilicity to modulate their thermoresponsiveness. Ethoxyl terminals on the dendrons were selected for affording the polymers with more hydrophobicity to have lower phase transition temperatures, while methoxyl terminals were designed to attribute the polymers with slightly higher hydrophilicity in order to exhibit higher phase transition temperatures. The branching densities of OEG dendrons were designed based on following considerations: (1) to have different overall hydrophilicity, with the 2-fold the highest hydrophobicity and the 6-fold the highest hydrophobicity, (2) to have different crowding effects from the collapsed OEGs around the PPA backbones, and (3) to have different steric hindrance for modulating the induction of backbone chirality. The synthesis of these dendronized PAs was processed with methods described in our previous reports through esterification and amidation with excellent yields. All new compounds were characterized by ^{1}H-NMR spectroscopy to confirm their structures (Figs. S1–S20 in the electronic supplementary information, ESI).

Thanks to the characteristic feature from dendritic OEGs,[49,50] these dendronized macromonomers are thermoresponsive, and the cloud points (T_{cp}s) of **Me-PA$_2$**, **Et-PA$_2$**, **Me-PA$_3$**, **Et-PA$_3$** and **Et-PA$_6$** were found to be 10.4, 14.3, 74.0, 22.0 and 45.0 °C, respectively, according to the turbidimetry (Fig. S21 in ESI). Above indicates that PA monomers carrying 2-fold dendritic OEG are quite hydrophobic with phase transition temperature below room temperature. PA monomer bearing 3-fold dendritic OEG with ethoxyl terminals exhibits modulate hydrophilicity with a phase transition temperature around room temperature. In contrast, that carrying 3-fold dendritic OEG with methoxyl terminals exhibits much higher hydrophilicity, and its phase transition temperature can be high as 74.0 °C. For the PA monomer pendanted with 6-fold OEG dendron, its phase transition temperature is 45.0 °C, which is much higher than that (22.0 °C) for its counterparts with 3-fold dendritic OEG. This indicates branching density of the OEG chains also contribute hydrophilicity to the dendritic macromonomers.

Polymerization in Various Solvents

Polymerization of these dendronized PAs catalyzed by $[Rh(nbd)Cl]_2$ at room temperature afforded corresponding dendronized PPAs. Here, effects of polymerization solvents on the polymerization process were examined, focusing on their possible influence on thermoresponsiveness and chirality of obtained polymers. Both **Me-PA$_2$** and **Et-PA$_2$** show strong hydrophobic, and their polymerizations can only be processed

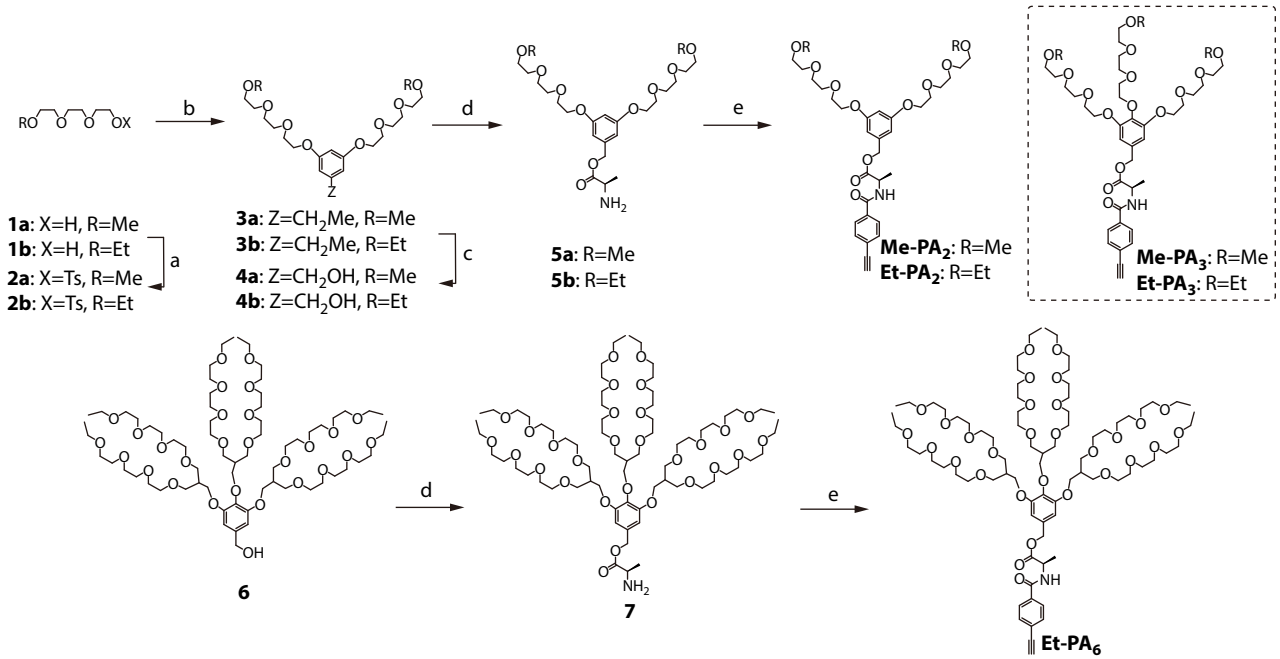

Scheme 1 Synthetic procedure for dendronized macromonomers **Me-PA$_2$**, **Et-PA$_2$** and **Et-PA$_6$**. For easy comparison, molecular structures of **Me-PA$_3$** and **Et-PA$_3$** were included. Reagents and conditions: (a) TsCl, **1a** or **1b**, NaOH, THF, 0 °C, 12 h (86% for **2a**, 84% for **2b**); (b) 3,5-Dihydroxybenzoic acid, **2a** or **2b**, K_2CO_3, DMF, 80 °C, 24 h (90% for **3a**, 85% for **3b**); (c) $LiAlH_4$, **3a** or **3b**, THF, 0 °C, 12 h (86% for **4a**, 88% for **4b**); (d) L-Boc-Ala-OH, **4a** or **4b** or **6**, DMAP, EDC, DCM, TFA, 0 °C, 24 h (74% for **5a**, 82% for **5b**, 90% for 7); (e) Perfluorophenyl 4-ethynylbenzoate, **5a** or **5b** or **7**, DIEA, DCM, 0 °C, 24 h (82% for **Me-PA$_2$**, 51% for **Et-PA$_2$**, 83% for **Et-PA$_6$**). Abbreviations: DCM = dichloromethane, DIEA = *N*,*N*-diisopropylethylamine, DMAP = 4-(dimethylamino)pyridine, EDC = 1-(3-dimethylaminopropyl)-3-ethylcarbodiimide, TFA = trifluoroacetic acid, THF = tetrahydrofuran.

https://doi.org/10.1007/s10118-023-2991-6

in organic solvents. Differently, PA monomers carrying either 3-fold or 6-fold dendritic OEGs are well-soluble in both water and organic solvents. Therefore, their polymerizations were performed in water, THF and methanol, and the obtained dendronized PPAs were named with a footnote as followings: W for water, T for THF, and M for methanol. The polymerization results are summarized in Table 1. PPAs with modulated molar masses were obtained, which are relevant to certain degree to polymerization solvents. Polymerization in water which is not a good solvent to the monomers always afford polymers higher molar masses when comparing to these polymers from good solvents like THF and methanol. AFM images in Fig. 2 show that these dendronized PPAs adopt worm-like chain morphology with chain lengths in the range of a few hundred of nanometers, and these with 6-fold dendrons are slightly thicker and more rigid than these carrying 3-fold dendrons.

Thermoresponsiveness of the Dendronized PPAs

PPAs carrying 2-fold dendritic OEGs are not water-soluble, indicating their strong hydrophobicity. Differently, dendronized PPAs with both 3-fold and 6-fold dendritic OEGs are all soluble in water at room temperature. However, their solubilities are different, and related to branching densities of the OEG dendrons and to the polymerization conditions. PPAs carrying 3-fold OEG dendrons normally required much longer time to be dissolved in water when compared to these carrying 6-fold OEG dendrons, suggesting higher branching densities of OEG chains enhanced the dissolution. These dendronized PPAs from polymerization in different solvents also exhibit different solubilities, and their water solubilities are in the order as following: **Et-PPA$_{6T}$** > **Et-PPA$_{6M}$** > **Et-PPA$_{3T}$** ≈ **Et-PPA$_{3M}$** > **Et-PPA$_{6W}$** > **Et-PPA$_{3W}$**. Polymers **Et-PPA$_{6W}$** and **Et-PPA$_{3W}$** through polymerization in aqueous solutions required much longes time to dissolve when compared to their counterparts through polymerization in organic solvents. For **Et-PPA$_{3W}$**, its aqueous solution even contained some flocculent insoluble matter. Since all **Et-PPA$_3$** obtained through polymerization in different solvents have exact the same molecular structure, their different solubility should be originated from their different conformations. In other words, the above results imply that PPAs obtained in aqueous phase adopted different molecular conformations. At elevated temperatures, their yellowish aqueous solutions turned into turbid due to dehydration and collapse of the dendritic OEGs, indicating their thermoresponsiveness.

Turbidimetry by using UV-Vis spectrophotometer was performed to investigate their thermoresponsive behavior, and the turbidity curves are shown in Fig. 3. Polymers carrying 3-fold dendritic OEGs obtained through polymerization in organic solvents, **Et-PPA$_{3T}$** and **Et-PPA$_{3M}$**, exhibit characteristic thermally-induced aggregation behavior, and their turbidity curves are quite sharp and hystereses between heating-cooling are small. T_{cp}s of **Et-PPA$_{3T}$** and **Et-PPA$_{3M}$** are 32.5 and 30.0 °C, respectively. However, for **Et-PPA$_{3W}$**, which was obtained from polymerization in water, its turbidity curves indicate its weak thermally mediated aggregation. Even at elevated temperature, solution of this polymer remained turbid with a transmittance around 60% but without obvious phase transition as shown in Fig. 3. This suggests that thermally-induced collapse of this polymer is not able to drive the intensive aggregation to form more dense aggregates. For the counterparts with methoxyl terminals, **Me-PPA$_{3T}$**, **Me-PPA$_{3W}$** and **Me-PPA$_{3M}$**, are much hydrophilic, their turbidity curves are much broader, and their T_{cp}s are 75.1, 60.6 and 59.9 °C, respectively. It is necessary to point out that **Me-PPA$_{3W}$** obtained through polymerization in water exhibited the expected phase transition only when its solution concentration is as high as 2.0 mg·mL^{-1}, indicating thermally-induced aggregation of this polymer required high concentration to compensate for the weak aggregation kinetics. For PPAs with 6-fold dendritic OEGs, they are slightly hydrophilic than these with 3-fold dendritic OEGs. **Et-PPA$_{6T}$** exhibited normal thermal dehydration and aggregation with a slight broad phase transition at T_{cp}=35.5 °C. Differently, neither **Et-PPA$_{6M}$** nor **Et-PPA$_{6W}$** show the expected thermoresponsive behavior. Above indicates that branching densities of OEG chains in the dendron pendants around the PPA backbones play an important role in mediating the thermally-dehydration and aggregation. Densely packed hydrophilic OEGs in PPAs with 6-fold dendritic OEGs provide enhanced shielding effects to the hydrophobic PPA backbones, affording the polymers enhanced hydrophilicity.

Thermoresponsiveness of the dendronized PPAs were fur-

Table 1 Polymerization conditions and characterization results of the polymers. [a]

Polymers	Monomer	Solvent	Yield (%)	GPC results [b]		T_{cp} [c] (°C)
				M_n (×10^{-4})	$Đ$	
Me-PPA$_{2T}$	**Me-PA$_2$**	THF	72	11.2	1.95	–
Et-PPA$_{2T}$	**Et-PA$_2$**	THF	60	35.1	1.90	–
Me-PPA$_{3T}$	**Me-PA$_3$**	THF	86	17.0	1.60	75.1
Me-PPA$_{3W}$	**Me-PA$_3$**	Water	85	54.6	2.27	60.6 [d]
Me-PPA$_{3M}$	**Me-PA$_3$**	MeOH	71	62.9	1.96	59.9
Et-PPA$_{3T}$	**Et-PA$_3$**	THF	85	38.6	2.13	32.5
Et-PPA$_{3M}$	**Et-PA$_3$**	MeOH	89	61.4	1.98	30.0
Et-PPA$_{3W}$	**Et-PA$_3$**	Water	94	79.4	1.38	–
Et-PPA$_{6T}$	**Et-PA$_6$**	THF	87	22.9	2.52	35.5
Et-PPA$_{6M}$	**Et-PA$_6$**	MeOH	89	22.1	2.62	–
Et-PPA$_{6W}$	**Et-PA$_6$**	Water	91	42.6	2.01	–

[a] Polymerization with [Rh(nbd)Cl]$_2$ as catalysts in the presence of TEA at room temperature for 12 h; [b] Determined by GPC with DMF as eluent containing 0.1 wt% LiBr calibrated with PMMA standards; [c] Apparent T_{cp}s of the polymers were determined as the temperature at 50% of the initial transmittance at λ=700 nm, C=0.5 mg·mL^{-1}; [d] C=2.0 mg·mL^{-1}.

https://doi.org/10.1007/s10118-023-2991-6

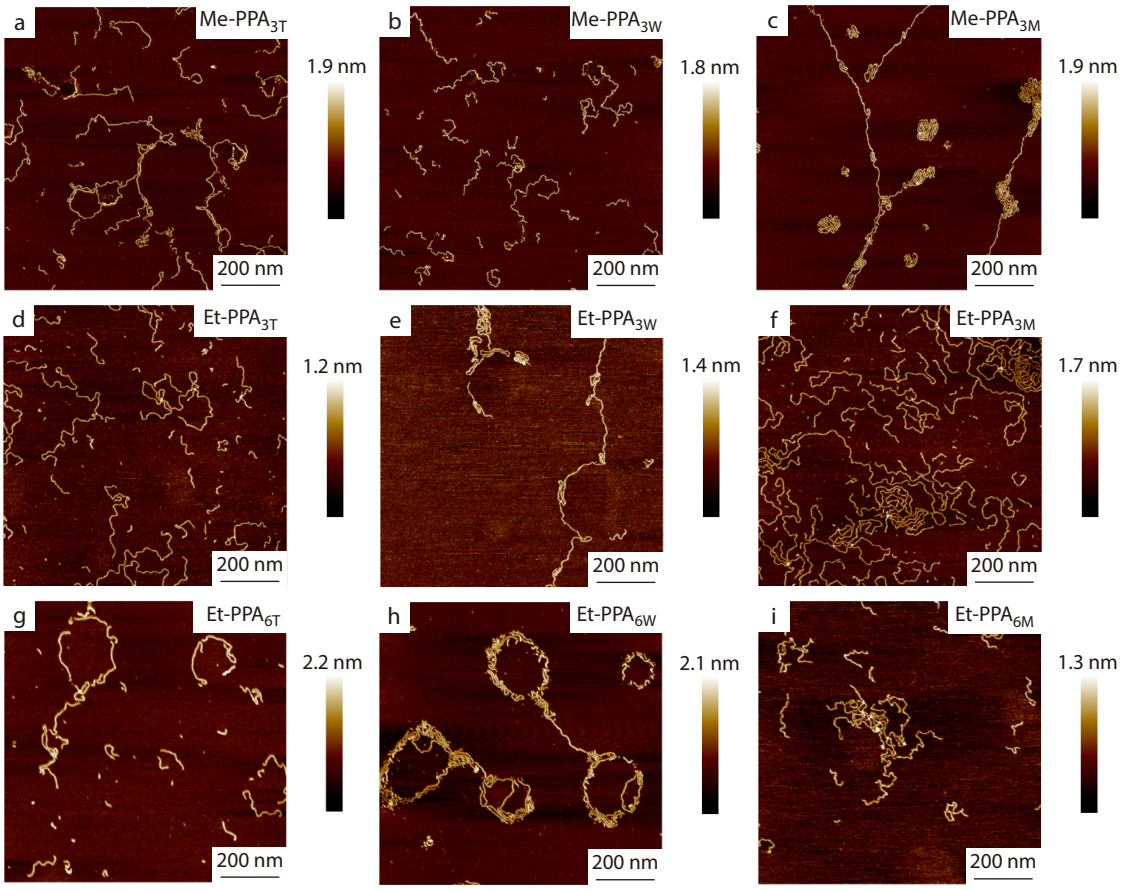

Fig. 2 AFM images of the dendronized PPAs on mica: (a) **Me-PPA$_{3T}$**, (b) **Me-PPA$_{3W}$**, (c) **Me-PPA$_{3M}$**, (d) **Et-PPA$_{3T}$**, (e) **Et-PPA$_{3W}$**, (f) **Et-PPA$_{3M}$**, (g) **Et-PPA$_{6T}$**, (h) **Et-PPA$_{6W}$** and (i) **Et-PPA$_{6M}$**. Samples were prepared through spinning coating from $CHCl_3$ solutions on mica at room temperature. C=0.005 mg·mL^{-1}.

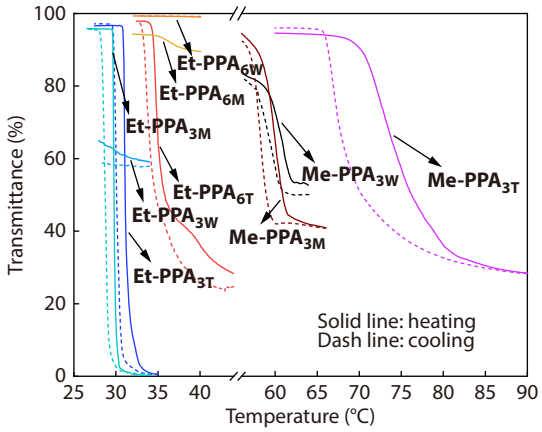

Fig. 3 Plot of transmittance versus temperature for aqueous solutions of the dendronized PPAs. For **Me-PPA$_{3W}$**, C=2 mg·mL^{-1}, while for the others, C=0.5 mg·mL^{-1}.

ther explored by temperature-varied ^{1}H-NMR spectroscopy. As shown in Fig. S22 (in ESI), with increase of temperature, proton signals from **Et-PPA$_{3T}$**, **Et-PPA$_{3M}$** and **Et-PPA$_{6T}$** corresponding to the OEGs (chemical shift 3.5 or so) became broad obviously, and their intensities reduced simultaneously. However, the proton signals corresponding to OEG moieties and their intensities from **Et-PPA$_{3W}$**, **Et-PPA$_{6W}$** and **Et-PPA$_{6M}$** did not change significantly with the increase of temperature, indicating that no obvious temperature-induced dehydration collapse occurred for these dendronized PPAs. This result is in good agreement with the findings from turbidimetry as discussed above.

Effects of polymerization solvents on thermoresponsiveness of the resulting polymers indicate that the solvent exhibited influence on the propagation of polymer chains and the packing of dendritic OEGs around the PPA backbones. In bad solvent water, dendritic macromonomers may have pre-aggregated to certain degree due to their amphiphilicity, and the polymerization processed among the aggregates instead of the monomers, which led to the formation of PPA backbones with highly structured and densely assembled. This may prevent the dehydration and collapse of the dendritic OEGs. Interestingly, polymers obtained from polymerization in different solvents showed a strong memory for their different thermoresponsive behavior. After polymerization, these polymers were purified with organic solvent DCM, which is a good solvent to all dendronized PPAs. However, the different thermoresponsive behavior was retained. Further experiments were performed to illustrate the high stability for the configurations. For example, **Et-PPA$_{3W}$**, **Et-PPA$_{6W}$** and **Et-PPA$_{6M}$** were dissolved in THF and stood for 3 days. After the organic solvent was removed, they were re-dissolved in water for testing. It was found that they still had no thermore-

https://doi.org/10.1007/s10118-023-2991-6

sponsive behavior. Therefore, the polymer configuration from the effects of the polymerization solvents retained in all polymers. In other words, the configuration of the dendronized PPAs obtained in various solvents is quite stable.

Possible aggregation of the dendronized PPAs from different solvents was followed with DLS measurements. Hydrodynamic radii (R_hs) of **Et-PPA$_{3T}$**, **Et-PPA$_{3M}$** and **Et-PPA$_{6T}$** at low temperatures are about 60, 110 and 70 nm, respectively. When the temperature increased above their T_{cp}s, R_hs of **Et-PPA$_{3T}$**, **Et-PPA$_{3M}$** and **Et-PPA$_{6T}$** increased to about 130, 140 and 100 nm, respectively. These results once again proved that **Et-PPA$_{3T}$**, **Et-PPA$_{3M}$** and **Et-PPA$_{6T}$** have obvious temperature-induced aggregation. However, it is necessary to point out that, at room temperature, R_hs of these dendronized PPAs were all above 60 nm, much larger than the single chain molecular sizes corresponding to their molecular weights,[51] indicating that these dendronized PPAs tend to aggregate at room temperature. For the polymers failed to show thermoresponsiveness, R_hs of **Et-PPA$_{3W}$**, **Et-PPA$_{6W}$** and **Et-PPA$_{6M}$** in water are 110, 75 and 110 nm, respectively. Their R_gs decreased gradually with increase of temperature, indicating the aggregates at low temperature were shrank upon heating. Above results suggest that the dendronized PPAs are amphiphilic, with the pendanted OEG dendrons hydrophilic and the PPA backbones hydrophobic. This radial amphiphilicity within the worm-like molecular objects provides driving force for them to aggregate and even assemble in selective solvents.

Chiroptical Properties of the Dendronized PPAs

Aqueous solutions of the dendronized PPAs show difference colors, which is dependent on branching densities of the OEG dendrons and the polymerization solvents. As shown in Fig. 4(a), the colors from PPAs carrying 6-fold dendritic pendants are always deeper than those with 3-fold dendritic pendants. In addition, the solution of **Et-PPA$_{3W}$** obtained through polymerization in water show the weakest color at the same concentration, indicating the selective solvent water is not in favor of forming PPAs with longer conjugated backbones. As revealed previously in reports from Tabata *et al*., solution color of PPAs may reflect tacticity differences of the polymer backbones, which may be also related to the PPA chirality.[40] Therefore, chiralities of these dendronized PPAs were first investigated by CD spectroscopy, and exhibit different chiralities in difference solvents. As shown in Fig. 4, the strongest positive Cotton effects at 375 nm corresponding to the PPA backbone can be observed from PPA carrying 3-fold dendritic pendants through polymerization in methanol. For its counterparts obtained through polymerization in water or THF, modulated Cotton effects can be observed in solvent of methanol (Fig. 4b), THF (Fig. 4c) or DCM (Fig. 4d). This indicates that chiralities of these dendronized PPAs are related to the polymerization solvents. Since all polymers after the polymerization were

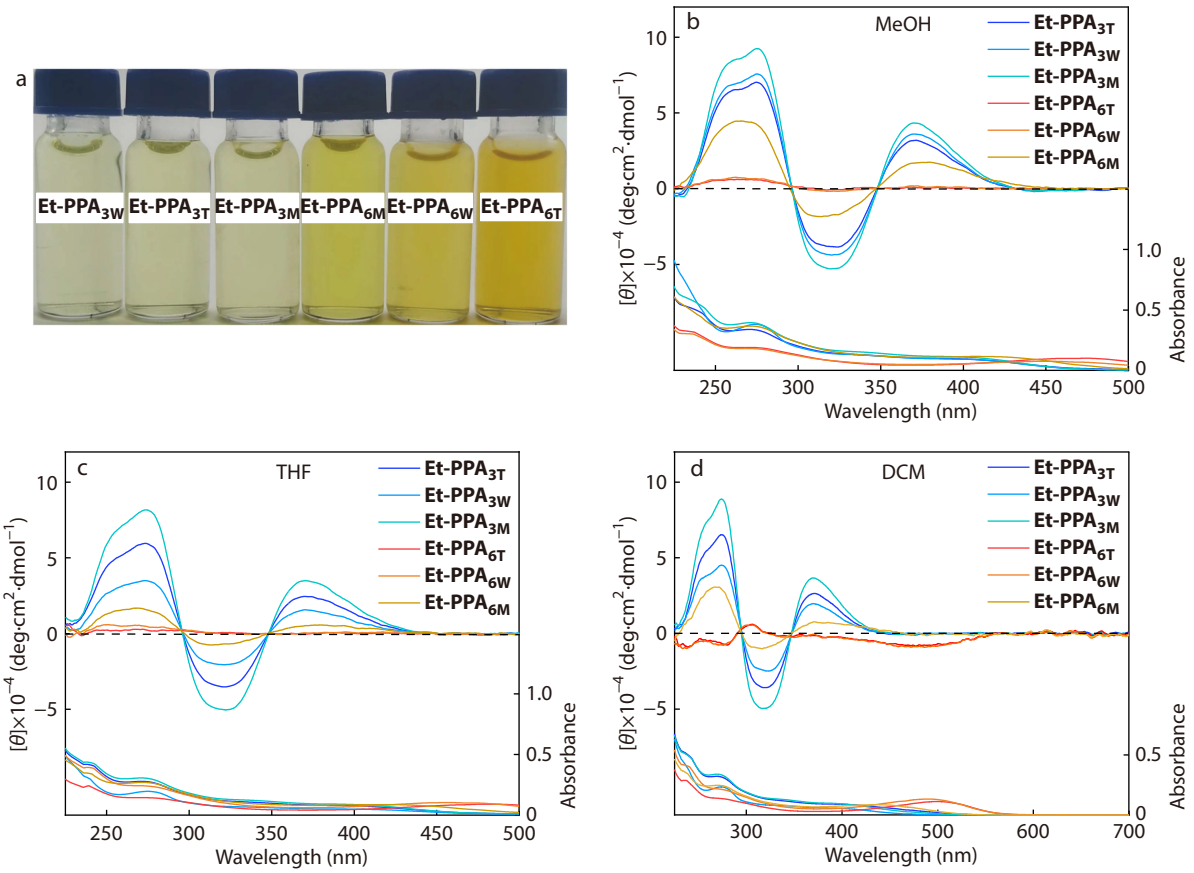

Fig. 4 Photographs of aqueous solutions of the dendronized PPAs at (a) 25 °C, as well as CD and UV-Vis spectra of PPAs in (b) MeOH, (c) THF and (d) DCM at 25 °C. C=0.25 mg·mL^{-1}.

https://doi.org/10.1007/s10118-023-2991-6

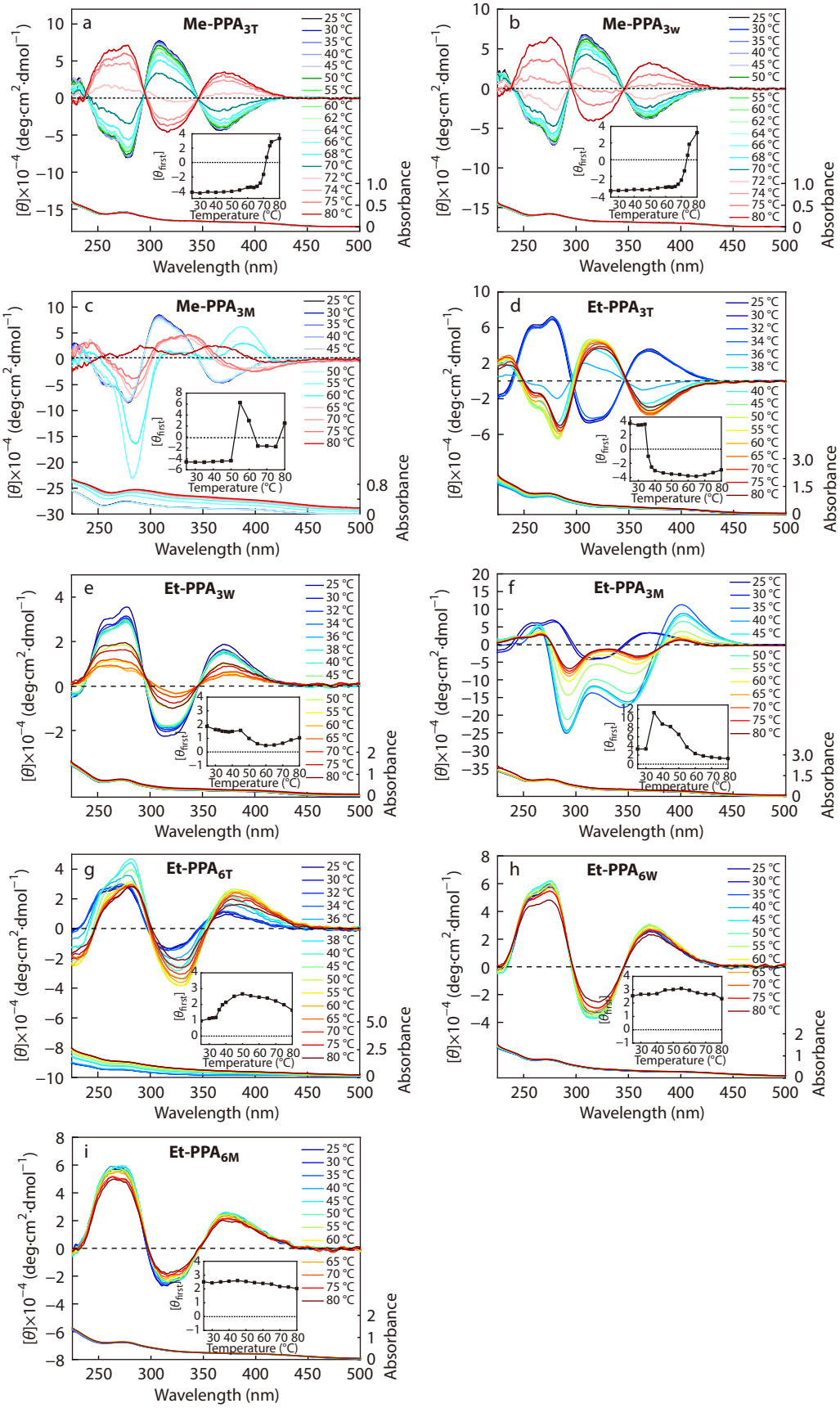

Fig. 5 Temperature-variable CD and UV-Vis spectra of (a) **Me-PPA$_{3T}$**, (b) **Me-PPA$_{3W}$**, (c) **Me-PPA$_{3M}$**, (d) **Et-PPA$_{3T}$**, (e) **Et-PPA$_{3W}$**, (f) **Et-PPA$_{3M}$**, (g) **Et-PPA$_{6T}$**, (h) **Et-PPA$_{6W}$**, (i) **Et-PPA$_{6M}$** in H_2O. *C*=0.25 mg·mL^{-1}.

https://doi.org/10.1007/s10118-023-2991-6

purified through column chromatography with DCM as eluent and freezing dried before all measurements, the retained chirality difference for the polymers from different polymerization solvents suggests that the chiralities originated from polymerization were memorized, no matter what kind of treatment history (purification, drying, and dissolution in organic solvent) was applied. Differently, PPAs carrying 6-fold dendritic OEG pendants obtained through polymerization in water or THF always showed very weak Cotton effects in the wavelength range corresponded to the backbone, no matter what solvent was used for the measurements. This suggests the 6-fold dendritic pendants may have provided too much steric hindrance for the backbone to adopt ordered chiral structures.

Based on the characteristic thermoresponsive feature of these dendronized PPAs, temperature-varied CD and UV-Vis spectra of their aqueous solutions were carried out, aiming at exploring the chiroptical properties during the thermally-induced phase transitions. The resulted CD spectra with plots of the first peak intensities against temperature as inset are shown in Fig. 5. For dendronized PPAs with the hydrophilic methoxyl terminals, **Me-PPA$_{3T}$** (Fig. 5a) and **Me-PPA$_{3W}$** (Fig. 5b), typical helical conformation inversion across their T_{cp}s can be observed. Similar to thermoresponsive PPAs,[39,44] these polymers changed their helicity from left-handed to right-handed. Well below their T_{cp}s, the negative Cotton effect at 375 nm remains unchange as temperature increasing. However, when solution temperature reaches their T_{cp}s, the negative Cotton signal intensities reduce with the increase of temperature. Further increase of solution temperature above the T_{cp}s led to appearance of a positive Cotton signal, whose intensities increased with temperature. Here, polymerization solvent exhibits negligible effect on their thermally-dehydration mediated chirality transitions, since both **Me-PPA$_{3T}$** and **Me-PPA$_{3W}$** show exactly the same chirality transitions during the temperature variation across their T_{cp}s.

For dendronized PPAs with the hydrophobic ethoxyl terminals, **Et-PPA$_{3T}$** (Fig. 5d), **Et-PPA$_{3W}$** (Fig. 5e) and **Et-PPA$_{3M}$** (Fig. 5f), their Cotton signals change in different ways when temperature varied across their T_{cp}s. For **Et-PPA$_{3T}$**, as we illustrated previously, Cotton effect at 375 nm remains unchange when temperature was below its T_{cp} (~34.0 °C). However, the CD intensity at 375 nm sharply decreases when increasing temperature close to T_{cp}. Above its T_{cp}, Cotton effect passes zero, and further increase of solution temperature affords Cotton effect to have a negative value, which remains almost unchange. This Cotton signal inversion indicates **Et-PPA$_{3T}$** changed from right-handed helical conformation into left one. Similarly, both **Et-PPA$_{3W}$** and **Et-PPA$_{3M}$** also adopted right-handed helical conformations at room temperature. However, their Cotton effects took different transition fashions during the thermally-mediated phase transitions. For **Et-PPA$_{3W}$**, the Cotton signal intensity at 375 nm reduces when solution temperature increases across its T_{cp}, but no inversion happened. For **Et-PPA$_{3M}$**, the Cotton signal increased its intensity significantly when solution temperature increased across its T_{cp} with a large red-shift from 375 nm to 402 nm (Δ=27 nm). Obvious different chirality transitions during the thermally-induced phase transitions for polymers **Et-PPA$_{3T}$**, **Et-PPA$_{3W}$** and **Et-PPA$_{3M}$** suggest that these dendronized PPAs obtained through polymerization in different solvents should have different tacticity and adopted different chain conformations. Monomers in selective solvents like water or methanol should have aggregated to some degree, which made the polymerizations happened within the aggregates. This should lead to different chain conformation, and overall hydrophilicity of the resulting polymers. Effects of polymerization solvents on thermoresponsiveness and chiralities of the resulted dendronized PPAs may also be related to different solvation of Rh catalyst during the polymerization. Solvent like water, MeOH and THF may also act as donor to interaction with the Rh catalyst against the original ligand nbd, exhibiting different catalysis activities and leading to different backbone tacticity.

As illustrated in Fig. 6, polymerization solvents show influ-

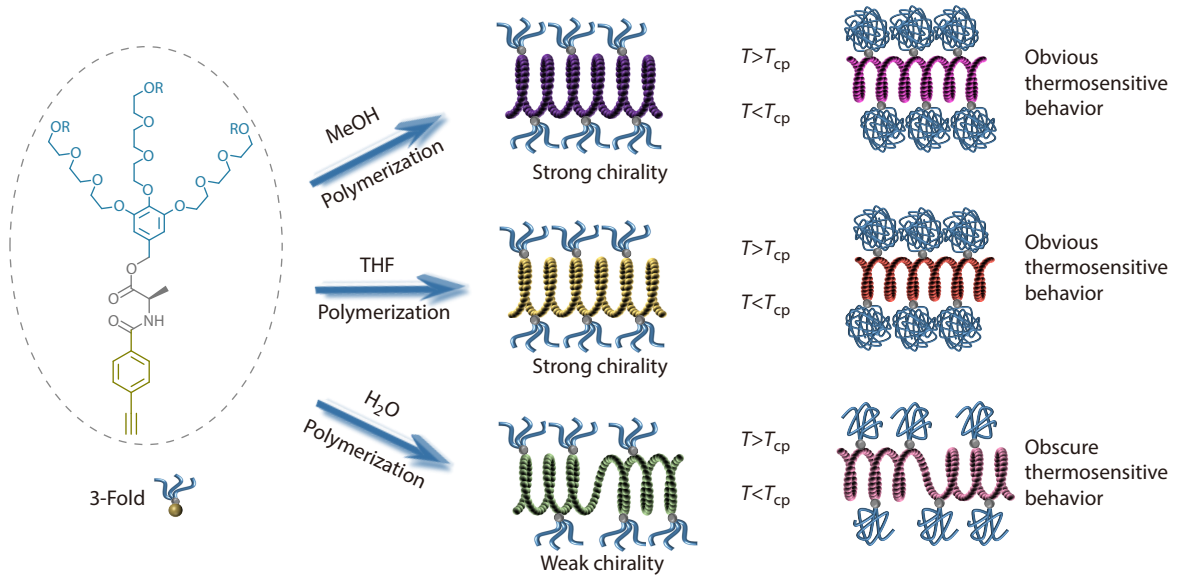

Fig. 6 Illustration of effects of polymerization solvents on thermoresponsiveness and helicity of dendronized PPA carrying 3-fold dendritic OEGs.

https://doi.org/10.1007/s10118-023-2991-6

ence not only on the chiralities of the obtained dendronized PPAs, but also on their thermoresponsive behavior. For dendronized PPAs carrying much bulky 6-fold dendritic OEG pendants, **Et-PPA$_{6T}$** (Fig. 5g), **Et-PPA$_{6W}$** (Fig. 5h) and **Et-PPA$_{6M}$** (Fig. 5i), their weak Cotton effects at 375 nm were much stable and their intensities changed only slightly when temperature increased across their T_{cp}s. This may be originated from the high steric hindrance from 6-fold dendritic OEG pendants. Certainly, sufficient shielding from the bulky 6-fold dendron to the interiors of the PPA main chains may be supportive to prevent them from strong solvation, which should be a key issue for the stability of a helical polymers. When solution temperature was cooled down to room temperature, the original CD spectra were restored, indicating chirality transformation of these dendronized PPAs mediated by thermally induced aggregation is fully reversible. The above results are consistent with the observations in our previous reports.

CONCLUSIONS

A homologous series of dendronized PPAs with worm-like chain morphology were prepared by homopolymerization of the dendritic macromonomers with Rh catalyst in different solvents. These macromonomers carry 2-fold, 3-fold and 6-fold dendritic OEGs, respectively, and the different branching densities of OEG chains were found to play important role in mediating thermoresponsiveness and chiroptical properties of the resulting polymers. Higher branching densities offered the polymer backbone better shielding, ensuring higher hydrophilicity of the polymers with either higher phase transition temperatures or deteriorated thermal aggregation behavior. At the same time, dendritic pendants with higher branching densities provided high steric hindrance in mediating the polymers stable chirality. Polymerization solvents (non-selective: THF, and selective: methanol and water) were found to play important role in modulating the thermoresponsiveness and helicity of the resulting polymers. Chirality difference for the polymers from different polymerization solvents was retained, no matter how these polymers were purified and what kind of solvents used for treatment after the polymerization. This indicates that the chiralities originated from polymerization in different solvents are very stable and have been memorized by the polymers. PPAs carrying different dendritic pendants offered the polymers different chirality transitions across their thermally-induced phase transitions. PPAs carrying methoxyl terminals inverted from left-handed into right-handed conformation after dehydrated and aggregated, and made sharp difference to their counterparts with ethoxyl terminals, which inverted their conformation from right-handed to left-handed when heated to the elevated temperatures. These findings are interesting, and are helpful for further understanding the relationship between topological structures, shielding effects to the polymer backbones, and their chirality. We therefore believe this work represents a motivation for deeper understanding between dendritic structures and chirality, which may open a new route for manipulating polymer's chirality and responsive properties.

Conflict of Interests

The authors declare no interest conflict.

Electronic Supplementary Information

Electronic supplementary information (ESI) is available free of charge in the online version of this article at http://doi.org/10.1007/s10118-023-2991-6.

ACKNOWLEDGMENTS

This work was financially supported by the National Natural Science Foundation of China (Nos. 21971160 and 21971161) and Program for Professor of Special Appointment (No. Eastern Scholar TP2019039) at Shanghai Institutions of Higher Learning.

REFERENCES

1 Okamoto, Y. Helical polymers for efficient enantiomer separation. *Adv. Polym. Sci.* **2013**, *261*, 391–414.
2 Leigh, T.; Fernandez-Trillo, P. Helical polymers for biological and medical applications. *Nat. Rev. Chem.* **2020**, *4*, 291–310.
3 Zhang, Y.; Deng, J. Chiral helical polymer materials derived from achiral monomers and their chiral applications. *Polym. Chem.* **2020**, *11*, 5407–5423.
4 Zheng, Z. G.; Lu, Y. Q.; Li, Q. Photoprogrammable mesogenic soft helical architectures: a promising avenue toward future chiro-optics. *Adv. Mater.* **2020**, *32*, 1905318.
5 Li, S. Y.; Gao, R. T.; Chen, Z.; Liu, N.; Wu, Z. Q. Advances in circularly polarized luminescence materials based on helical polymers. *J. Mater. Chem. C* **2023**, *11*, 1242–1250.
6 Nakano, T.; Okamoto, Y. Synthetic helical polymers: conformation and function. *Chem. Rev.* **2001**, *101*, 4013–4038.
7 Liu, J. Z.; Lam, J. W. Y.; Tang, B. Z. Acetylenic polymers: syntheses, structures, and functions. *Chem. Rev.* **2009**, *109*, 5799–5867.
8 Scanga, R. A.; Reuther, J. F. Helical polymer self-assembly and chiral nanostructure formation. *Polym. Chem.* **2021**, *12*, 1857–1897.
9 Wen, T.; Wang, H. F.; Li, M. C.; Ho, R. M. Homochiral evolution in self-assembled chiral polymers and block copolymers. *Acc. Chem. Res.* **2017**, *50*, 1011–1021.
10 Zhang, L.; Wang, T.; Shen, Z.; Liu, M. Chiral nanoarchitectonics: towards the design, self-assembly, and function of nanoscale chiral twists and helices. *Adv. Mater.* **2016**, *28*, 1044–1059.
11 Bisoyi, H. K.; Li, Q. Light-directed dynamic chirality inversion in functional self-organized helical superstructures. *Angew. Chem. Int. Ed.* **2016**, *55*, 2994–3010.
12 Leiras, S.; Freire, F.; Quiñoá, E.; Riguera, R. Reversible assembly of enantiomeric helical polymers: from fibers to gels. *Chem. Sci.* **2015**, *6*, 246–253.
13 Yashima, E.; Maeda, K.; Iida, H.; Furusho, Y.; Nagai, K. Helical polymers: synthesis, structures and functions. *Chem. Rev.* **2009**, *109*, 6102–6211.
14 Freire, F.; Quiñoá, E.; Riguera, R. Supramolecular assemblies from poly(phenylacetylene)s. *Chem. Rev.* **2016**, *116*, 1242–1271.
15 Rey-Tarrio, F.; Guisan-Ceinos, S.; Cuerva, J. M.; Miguel, D.; Ribagorda, M.; Quinoa, E.; Freire, F. Photostability and dynamic helical behavior in chiral poly(phenylacetylene)s with a preferred screw-sense. *Angew. Chem. Int. Ed.* **2022**, *61*, 202207623.
16 Yashima, E.; Maeda, K. Chirality-responsive helical polymers. *Macromolecules* **2008**, *41*, 3–12.
17 Okamoto, Y.; Nakano, T. Asymmetric polymerization. *Chem. Rev.* **1994**, *94*, 349–372.

18 Zhang, A.; Ropero, F. R.; Zanuy, D., Alemán, C.; Meijer, E.; Schlüter, A. A rigid, chiral, dendronized polymer with a thermally stable, right-handed helical conformation. *Chem. Eur. J.* **2008**, *14*, 6924–6934.

19 Liu, K.; Zhang, X.; Tao, X.; Yan, J.; Kuang, G., Li, W., Zhang, A. Lysine-based dendronized polymers with preferred chirality. *Polym. Chem.* **2012**, *3*, 2708–2711.

20 Aoki, T.; Kaneko, T.; Maruyama, N.; Sumi, A.; Takahashi, M.; Sato, T.; Teraguchi, M. Helix-sense-selective polymerization of phenylacetylene having two hydroxy groups using a chiral catalytic system. *J. Am. Chem. Soc.* **2003**, *125*, 6346–6347.

21 Percec, V.; Aqad, E.; Peterca, M.; Rudick, J. G.; Lemon, L.; Ronda, J. C.; De, B. B.; Heiney, P. A.; Meijer, E. W. Steric communication of chiral information observed in dendronized polyacetylenes. *J. Am. Chem. Soc.* **2006**, *128*, 16365–16372.

22 Maeda, K.; Mochizuki, H.; Osato, K.; Yashima, E. Stimuli-responsive helical poly(phenylacetylene)s bearing cyclodextrin pendants that exhibit enantioselective gelation in response to chirality of a chiral amine and hierarchical super-structured helix formation. *Macromolecules* **2011**, *44*, 3217–3226.

23 Leiras, S.; Freire, F.; Seco, J.; Quinoa, E.; Ricardo, R. Controlled modulation of the helical sense and the elongation of poly(phenylacetylene)s by polar and donor effects. *Chem. Sci.* **2013**, *4*, 2735–2743.

24 Guan, X.; Wang, S.; Shi, G.; Zhang, J.; Wan, X. Thermoswitching of helical inversion of dynamic polyphenylacetylenes through *cis-trans* isomerization of amide pendants. *Macromolecules* **2021**, *54*, 4592–4600.

25 Xu, A.; Masuda, T.; Zhang, A. Stimuli-responsive polyacetylenes and dendronized poly(phenylacetylene)s. *Polym. Rev.* **2017**, *57*, 138–158.

26 Wamura, H.; Takeyama, Y.; Yamamoto, M.; Kurihara, H.; Morino, K.; Yashima, E. Chirality responsive helical poly(phenylacetylene) bearing L-proline pendants. *Chirality* **2011**, *23*, 35–42.

27 Sanda, F.; Shiotsuki, M.; Masuda, T. Controlled polymerization of phenylacetylenes using well-defined Rhodium catalysts. *Macromol. Symp.* **2015**, *350*, 67–75.

28 Motoshige, R.; Mawatari, Y.; Motoshige, A.; Yoshida, Y.; Sasaki, T.; Yoshimizu, H.; Suzuki, T.; Tsujita, Y.; Tabata, M. Mutual conversion between stretched and contracted helices accompanied by a drastic change in color and spatial structure of poly(phenylacetylene) prepared with a $[Rh(nbd)Cl]_2$-amine catalyst. *J. Polym. Sci., Part A: Polym. Chem.* **2014**, *52*, 752–759.

29 Miyagawa, T.; Furuko, A.; Maeda, K.; Katagiri, H.; Furusho, Y.; Yashima, E. Dual memory of enantiomeric helices in a polyacetylene induced by a single enantiomer. *J. Am. Chem. Soc.* **2005**, *127*, 5018–5019.

30 Maeda, K.; Mochizuki, H.; Watanabe, M.; Yashima, E. Switching of macromolecular helicity of optically active poly(phenylacetylene)s bearing cyclodextrin pendants induced by various external stimuli. *J. Am. Chem. Soc.* **2006**, *128*, 7639–7650.

31 Li, S.; Liu, K.; Kuang, G.; Masuda, T.; Zhang, A. Thermoresponsive helical poly(phenylacetylene)s. *Macromolecules* **2014**, *47*, 3288–3296.

32 Suarez-Picado, E.; Quinoa, E.; Riguera, R.; Freire, F. Poly(phenylacetylene) amines: a general route to water-soluble helical polyamines. *Chem. Mater.* **2018**, *30*, 6908–6914.

33 Cheuk, K.; Lam, J.; Lai, L.; Tang, B. Syntheses, hydrogen-bonding interactions, tunable chain helicities, and cooperative supramolecular associations and dissociations of poly(phenylacetylene)s bearing L-valine pendants: toward the development of proteomimetic polyenes. *Macromolecules* **2003**, *36*, 9752–9762.

34 Okoshi, K.; Sakurai, S. I.; Ohsawa, S.; Kumaki, J.; Yashima, E. Control of main-chain stiffness of a helical poly(phenylacetylene) by switching on and off the intramolecular hydrogen bonding through macromolecular helicity inversion. *Angew. Chem. Int. Ed.* **2006**, *45*, 8173–8176.

35 Sakurai, S. I.; Okoshi, K.; Kumaki, J.; Yashima, E. Two-dimensional surface chirality control by solvent-induced helicity inversion of a helical polyacetylene on graphite. *J. Am. Chem. Soc.* **2006**, *128*, 5650–5651.

36 Rodriguez, R.; Quinoa, E.; Riguera, R.; Freire F. Architecture of chiral poly(phenylacetylene)s: from compressed/highly dynamic to stretched/quasi-static helices. *J. Am. Chem. Soc.* **2016**, *138*, 9620–9628.

37 Sakai, R.; Satoh, T.; Kakuchi, T. Polyacetylenes as colorimetric and fluorescent chemosensor for anions. *Polym. Rev.* **2017**, *57*, 159–174.

38 Bergueiro, J.; Freire, F.; Wendler, E.; Seco, J. M.; Quinoa, E.; Riguera, R. The ON/OFF switching by metal ions of the "sergeants and soldiers" chiral amplification effect on helical poly(phenylacetylene)s. *Chem. Sci.* **2014**, *5*, 2170–2176.

39 Cao, Y.; Ren, L.; Zhang, Y.; Lu, X.; Zhang, X.; Yan, J.; Li, W.; Masuda, T.; Zhang, A. Remarkable effects of anions on the chirality of thermoresponsive helical dendronized poly(phenylacetylene)s. *Macromolecules* **2021**, *54*, 7621–7631.

40 Tabata, M.; Mawatari, Y. Emerging π-conjugated stretched and contracted helices and their mutual conversions of substituted polyacetylenes prepared using an organo-rhodium catalyst. *Polym. Rev.* **2017**, *57*, 65–88.

41 Fukushima, T.; Kimura, H.; Tsuchihara, K. Color and chiroptical control of poly(phenylacetylene) films with chiral hydroxyl group. *Macromolecules* **2009**, *42*, 8619–8626.

42 Yoshida, Y.; Mawatari, Y.; Motoshige, A.; Motoshige, R.; Hiraoki, T.; Wagner, M.; Müllen, K.; Tabata, M. Accordion-like oscillation of contracted and stretched helices of polyacetylenes synchronized with the restricted rotation of side chains. *J. Am. Chem. Soc.* **2013**, *135*, 4110–4116.

43 Motoshige, R.; Mawatari, Y.; Motoshige, A.; Yoshida, Y.; Sasaki, T.; Yoshimizu, H.; Suzuki, T.; Tsujita, Y.; Tabata, M. "Mutual conversion between stretched and contracted helices accompanied by a drastic change in color and spatial structure of poly(phenylacetylene) prepared with a $[Rh(nbd)Cl]_2$-amine catalyst". *J. Polym. Sci., Part A: Polym. Chem.* **2014**, *52*, 752–759.

44 Wang, F.; Zhou, C.; Liu, K.; Yan, J.; Li, W.; Masuda, T.; Zhang, A. Thermoresponsive dendronized poly(phenylacetylene)s showing tunable helicity. *Macromolecules* **2019**, *52*, 8631–8642.

45 Kim, Y.; Shin, S.; Lee, M. Development of toroidal nanostructures by self-assembly: rational designs and applications. *Acc. Chem. Res.* **2013**, *46*, 2888–2897.

46 Kouwer, P. H. J.; Koepf, M.; Le Sage, V. A. A.; Jaspers, M.; van Buul, A. M.; Eksteen-Akeroyd, Z. H.; Woltinge, T.; Schwartz, E.; Kitto, H. J.; Hoogenboom1, R.; Picken, S. J.; Nolte, R. J. M.; Mendes, E.; Rowan, A. E. Responsive biomimetic networks from polyisocyanopeptide hydrogels. *Nature* **2013**, *493*, 651–655.

47 Hu, G. X.; Li, W.; Hu, Y. L.; Xu, A. Q.; Yan, J. T.; Liu, L. X.; Zhang, X. C.; Liu, K.; Zhang, A. Water-soluble chiral polyisocyanides showing thermoresponsive behavior. *Macromolecules* **2013**, *46*, 1124–1132.

48 Xu, G.; Zhang, J.; Jia, R.; Li, W.; Zhang, A. Topological effects of dendronized polymers on their thermoresponsiveness and microconfinement. *Macromolecules* **2022**, *55*, 630–642.

49 Li, W.; Zhang, A.; Chen, Y.; Feldman, K.; Wu, H.; Schluter, A. D. Low toxic, thermoresponsive dendrimers based on oligoethylene glycols with sharp and fully reversible phase transitions. *Chem. Commun.* **2008**, 5948–5950.

50 Xu, G.; Zhang, J.; Qi, M.; Zhang, X.; Li, W.; Zhang, A. Thermoresponsive dendritic oligoethylene glycols. *Phys. Chem. Chem. Phys.* **2022**, *24*, 11848–11855.

51 Zhang, A.; Zhang, B.; Wachtersbach, E.; Schmidt, M.; Schluter, A. D. Efficient synthesis of high molar mass, first- to fourth-generation distributed dendronized polymers by the macromonomer approach. *Chem. Eur. J.* **2003**, *9*, 6083–6092.

https://doi.org/10.1007/s10118-023-2991-6